Desalination and Water Treatment
www.deswater.com
doi: 10.1080/19443994.2016.1140079

57 (2016) 24476–24486
November

Removal of Pb(II) ions from aqueous solutions by raw and alkali-treated *Degla Beida* stone

Abdelali Gherbia[a], Abdelmalek Chergui[a,b,*], Ahmed Réda Yeddou[a,c], Ammar Selatnia[a,b], Charlotte Hurel[d], Nicolas Marmier[d], Rabah Kerbachi[b], Boubekeur Nadjemi[a]

[a]*Laboratoire d'Etude et de Développement des Techniques de Traitement et d'Epuration des Eaux et de Gestion Environnementale LEDTEGE, Ecole Normale Supérieure, Kouba KOUBA BP 92, Algiers, Algeria, Tel. +213 21 52 25 28; Fax: +213 21 52 29 73; emails: abdelali98111@yahoo.fr (A. Gherbia), a_chergui@yahoo.fr (A. Chergui), aryeddou@yahoo.fr (A.R. Yeddou), ammarselatnia@yahoo.fr (A. Selatnia), bnadjemi@hotmail.com (B. Nadjemi)*
[b]*Ecole Nationale Polytechnique, Département Génie de l'Environnement, 10 Avenue Hassen Badi, BP 182, El Harrach, Algiers, Algeria, email: r_kerbachi@yahoo.fr (R. Kerbachi)*
[c]*Département de Génie de l'Environnement, Université de Boumerdes, 35000 Avenue de l'Indépendance, Boumerdes, Algeria*
[d]*Faculty of Sciences, University of Nice Sophia Antipolis, ECOMERS, Parc Valrose, 06108 Nice Cedex 02, France, emails: Charlotte.HUREL@unice.fr (C. Hurel), Nicolas.MARMIER@unice.fr (N. Marmier)*

Received 7 February 2015; Accepted 2 January 2016

ABSTRACT

The purpose of this work was to study the feasibility of removing Pb(II) ions from aqueous solutions using specific type of date stones, *Degla Beida* (DB), using batch adsorption technique. The characterization by FT-IR analysis before and after the treatment process, during this study, has shown the presence of different functional groups. scanning electron microscope was used to analyze the surface change of the DB stone before and after alkali treatment. Batch experiments were conducted in order to measure the effects of different parameters on adsorption of Pb(II) ions, such as pH, contact time, amount of adsorbent, and ionic strength ($CaCl_2$). The equilibrium adsorption data were interpreted using the Langmuir and Freundlich models, which shown that the Langmuir isotherm model fits the best with the highest determination coefficient R^2 value. The kinetic studies shown that the adsorption of the Pb(II) ions onto raw and alkali-treated DB stones correspond to a pseudo-second-order kinetic model.

Keywords: Adsorption; Kinetics; Isotherms; Lead (II) ions; Degla Beida stone

---

1. Introduction

Physical and chemical properties of lead such as softness, malleability, poor conductibility, and resistance to corrosion stimulate a lot of interest in many disciplines since a long time. This is due to the fact that these properties are suitable for a great variety of applications such as the storage capacity of batteries, military industry, water pipes, pigments and printing of books, manufacture of pesticides, precious metal recovery from cyanide, protective and antifouling paint, gasoline additives, and electronics industry [1,2]. Lead is a non-biodegradable and non-essential element. It is also one of the most ubiquitous pollutants and the second hazardous substance in terms of

---

*Corresponding author.

concentration. Numerous epidemiological studies have reported that the use and the distribution of lead and Pb-containing compounds in the environment are extremely dangerous to living organisms by ingestion or inhalation. This use can result in various and considerable consequences on human health such as chromosomal damage and risk of cancer, anemia, damages in the nervous system, enzyme inhabitation, generation of free hydrogen peroxide, impairment of learning and memory. Actually, deposited lead in bones can remain for years [3,4]. Therefore, lead has to be removed from wastewater to avoid this negative impact on the environment. Different physicochemical processes can be used for heavy metal removal, such as chemical precipitation, coagulation, flotation, ion exchange, filtration, electrochemical treatment, membrane filtration, reverse osmosis, and solvent extraction. However, these methods are much less efficient for concentrations below about 100 ppm [5,6,7].

Activated carbon is the most used adsorbent for wastewaters containing heavy metals. This is due to its high specific surface area. However, activated carbon is an expensive material because of the chemical and physical treatments used for its synthesis [8,9]. Therefore, various researches have investigated alternative adsorbents that might have a better efficiency on heavy metal ions and toxic organics, especially if the adsorbent is an inexpensive or zero price is available and can be used in place of activated carbon, such as raw agricultural solid waste including peach stones, olive stones, apricot stones, date stones, orange peel, almond shells, and rice husk [10–13]. According to FAO data of year 2003, Algeria is one of the largest date producers in the world with a yearly production of 492,000 tones. From this production, about 140,000 tones date stones are annually obtained. The stone is not a consumable part of date and is usually discarded as waste. On the other hand, there are few studies in the literature about the removal of non-biodegradable pollutants from wastewater using date stones.

The purpose of the present work was to validate the valorization of the *Degla Beida* (DB) stones as biosorbent for lead ions.

The ability of a biosorbent to accumulate a given pollutant is controlled by the physical and chemical properties of the biosorbent and of the adsorbing species, together with the operating conditions of the sorption process. Hence, the physical and chemical characteristics of raw (DB) and of the chemically treated with sodium hydroxide (NDB) DB stones were first investigated.

Batch biosorption tests were then performed under varying operating conditions to optimize the biosorption efficiency of DB stone (pH, contact time, amount of adsorbent, and ionic strength ($CaCl_2$)). Finally, the sorption data were compared with standard and equilibrium models to clarify the mechanisms that control lead ion biosorption.

2. Materials and methods

2.1. Adsorbent preparation

DB stone was obtained from Biskra region (southeast of Algeria). Prior to use, the DB stones were intensively washed with tap water to remove the soluble impurities from its surface and then naturally dried in sunlight. The samples were then crushed using a grinder crusher and washed with distilled water repeatedly until pH of the filtrate became steady. The sample was filtrated and dried in an oven at 60˚C for 24 h. Treated *Degla Beida* (NDB) was prepared by mixing the *raw* DB in 0.05 M sodium hydroxide NaOH solution for 4 h. The samples were then washed thoroughly with distilled water to remove the free sodium hydroxide. Then, the samples were filtrated and dried in oven at 60˚C for 24 h. Finally, the DB and NDB were sieved in order to obtain a particle size between 315 and 500 μm. Thereafter, the adsorbents were stored in a desiccator for further experimental use.

2.2. Adsorbent characterization

Chemical properties of DB and NDB samples were characterized using Fourier-transform infrared (FTIR) spectroscopy (Perkin Elmer FT-IR-Spectrometer 2000) from the scanning range of 500–4,000 cm^{-1}.

The amount of Al, Si, Ca, K, Na, Mg, Fe, and Mn, contained in DB and NDB (mg per kg adsorbent mass), was determined after acid digestion. About 0.500 g of each adsorbent DB and NDB was placed in Savillex Teflon bottles and digested using (3:2 HNO_3/HCl) at 200˚C on a hot plate. After cooling, centrifuging, and filtering, the digested samples were diluted to 50 mL with distillated water. The digestion experiment was repeated five times for each adsorbent. The concentration of Al, Si, Ca, K, Na, Mg, Fe, and Mn was determined by an inductively coupled plasma optical emission spectrometer (ICP-OES) Optima 7,300 DV. The PlasmaCAL multi-element standard solutions in 5% nitric acid were used to prepare appropriate elemental calibration standards.

Surface morphologies of DB and NDB were characterized by scanning electron microscope (SEM) at an accelerating voltage of 1.0 kV, a magnification of 300×, and a working distance of 15.3 mm.

2.3. Experimental

The stock solution of Pb(II) ions with a concentration of 1,000 mg L^{-1} was prepared by dissolving a quantity of 1.5985 g of $Pb(NO_3)_2$ (99.99%) (Alfa Aesar) in distilled water. All batch experiments were carried out by mixing 0.25 g of dried samples of untreated or treated adsorbent with 50 mL of aqueous solution of $Pb(NO_3)_2$. The effect of pH on Pb(II) ions adsorption was studied in the pH range between 2.0 and 8.0 at 25˚C. The pH was measured using a Consort C561-type pH-meter and was adjusted by adding micro-volumes of either 0.1 M NaOH or 0.1 M HCl. Further, the effect of the amount of adsorbent on the Pb(II) ions adsorption was studied for different initial adsorbent mass from 0.05 to 0.5 g, at a pH value of 4.7 and at a temperature of 25˚C. The effect of ionic strength ($CaCl_2$) on the Pb(II) ions adsorption was analyzed at concentrations equal to 0.01, 0.05, and 0.10 mol L^{-1}, with an initial concentration of Pb(II) ions equal to 100 mg L^{-1}. Finally, the lead adsorption isotherms were conducted by shaking for 24 h and using different initial concentrations of Pb(II) ions between 50 and 500 mg L^{-1} at a pH of 4.7. The flasks were rotated at 50 rpm using Labinco test-tube rotator. The concentration of Pb(II) ions in the solution was determined by an ICP-OES Optima 7300 DV at 220.353 nm.

The amount of Pb(II) ions adsorbed at equilibrium q_e (mg g^{-1}) was calculated using the following expression:

$$q_e = \frac{(C_0 - C_e)}{m} \times V \tag{1}$$

where C_0 and C_e are the liquid-phase concentrations of Pb(II) ions (mg L^{-1}) at initial and equilibrium, respectively. V is the volume of the solution (L), and m is the mass of adsorbent used (g). The percentage of lead ions adsorbed was evaluated as follows:

$$\text{Removal}(\%) = \frac{(C_0 - C_e)}{C_0} \times 100 \tag{2}$$

3. Results and discussion

3.1. Adsorbent characterization

3.1.1. FT-IR spectroscopy

The FT-IR spectra of the DB and NDB before and after alkali treatment are shown in Fig. 1. The intense absorption bands of DB at 3425.3 cm^{-1} indicate the presence of hydroxyl groups O–H and N–H. The peak at 2925.8 cm^{-1} corresponds to the C–H stretching vibration which indicates the presence of alkane functional groups. The peak at 2854.5 cm^{-1} is assigned to aliphatic C–H stretching in CH_3. The peak at 1747.4 cm^{-1} corresponds to the C=O stretching and can be attributed to the hemicelluloses and lignin. The strong absorption band at 1384.8 cm^{-1} indicates the asymmetrical bending vibration of CH_3 and CH_2. The peak at 1037.6 cm^{-1} can be assigned to the C–O stretching vibration of carboxylic acid and alcohols. On the other hand, from the FT-IR spectrum of NDB, the disappearance of the peaks at 2925.8, 2854.5, 1747.4, and 1037.6 cm^{-1} after alkali treatment proves that lignin was removed during the alkali treatment [14,15]. The appearance of several new bands at 3755.1, 3676.1, 3652.9, and 3433.1 cm^{-1} can be explained by the presence of hydroxyl groups O–H in NDB.

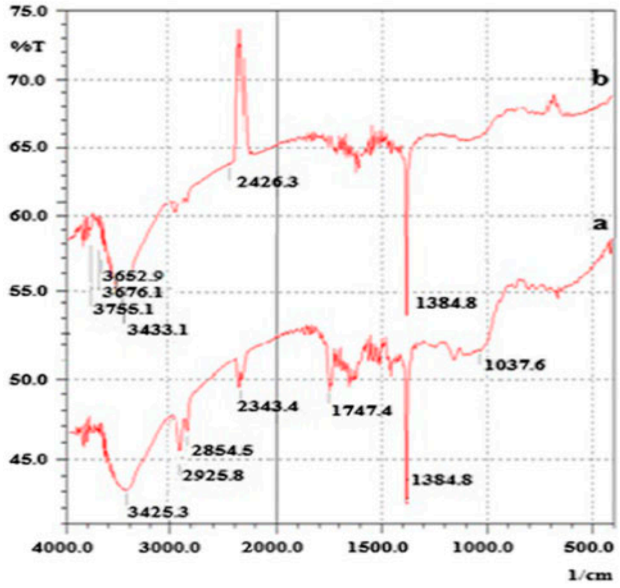

Fig. 1. FTIR spectra of DB (a) and NDB (b).

3.1.2. Elemental composition

The elemental composition of DB and NDB obtained from acid digestion is shown in Table 1. The predominant elements in the DB samples are calcium (Ca) and magnesium (Mg). In the NDB samples, the sodium (Na) and the calcium (Ca) constituted the largest elemental composition.

Table 1
Elemental composition of DB and NDB obtained from acid digestion

	Element (mg kg^{-1})							
Adsorbent	Al	Si	Ca	K	Na	Mg	Fe	Mn
DB	12.73 ± 0.15	14.22 ± 0.22	268.31 ± 0.17	37.11 ± 1.12	41.03 ± 0.33	85.53 ± 1.02	27.72 ± 0.62	ND
NDB	10.02 ± 1.32	10.18 ± 0.62	147.08 ± 0.53	13.26 ± 1.38	423.42 ± 1.66	29.84 ± 0.18	09.31 ± 0.10	ND

Note: ND = Not detected.

3.1.3. Scanning electron microscope

The microstructures of the DB and NDB were observed by SEM. They are shown in Fig. 2. As it can be seen, there is difference between the surface morphology of the samples. The treated adsorbent NDB has a rough surface with pores compared to the untreated adsorbent DB. This difference could be related to the removing of lignin during the treatment with sodium hydroxide.

3.2. Effect of adsorbent dose on Pb removal

The amount of used adsorbent plays an important role in adsorption process [16]. The effect of this parameter on the percentage and adsorption capacity of Pb(II) ions removal is illustrated in Fig. 3. It can be seen that for an increase in adsorbent dose from 1 to 10 g L^{-1}, the percentage of Pb(II) ions removal increases from 13.67 to 82.94% and from 30.03 to 97.52% for the DB and the NDB, respectively. This effect can be due to increase in adsorbent surface area and availability of more adsorption active sites which both stimulate more Pb(II) ions attached to their surfaces [17–19]. However, the amount of metal ions per mass unit of the adsorbent decreased from 13.67 to 8.29 mg g^{-1} and from 30.03 to 9.75 mg g^{-1} for the DB and NDB, respectively, at a constant values of Pb(II) ions concentration and volume. This may be due to the overlapping and aggregation of binding sites. Some of the binding sites could also remain unsaturated during the adsorption process when adsorbent amount increased [20,21].

3.3. Effect of contact time on Pb adsorption

In order to study the change in lead ions adsorption with time, the adsorption of the lead ions onto DB and NDB was measured as a function of contact time. As shown in Fig. 4, it can be clearly seen that the amount of lead ions adsorbed, using both adsorbents, increases with increasing contact time.

Fig. 4 shows also three important phases in the adsorption process. In the first phase, during the first 20 min, the adsorption rate of Pb(II) ions for both adsorbents is rapid. Actually, about 33.41 and 90.11% of the removal was achieved using the raw adsorbent and the treated adsorbent, respectively. In the second phase, the adsorption begins to slow and there is no significant increase. In the third phase, the equilibrium is reached after around 90 min for both DB and NDB,

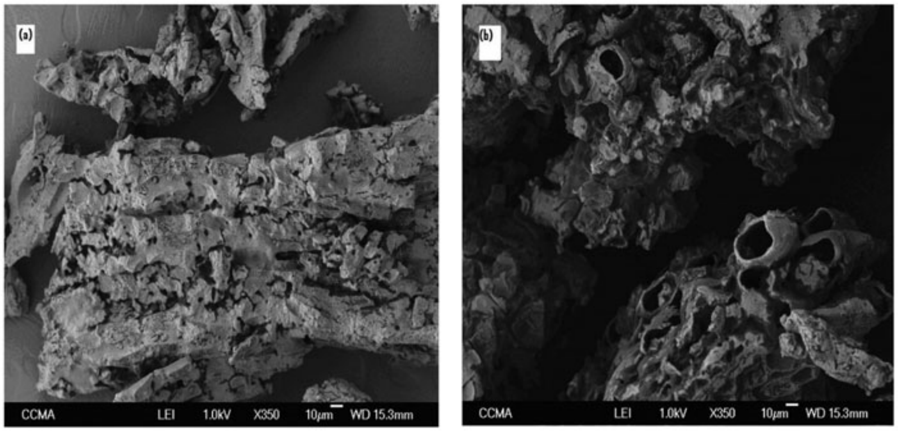

Fig. 2. SEM micrographs of DB (a) and NDB (b).

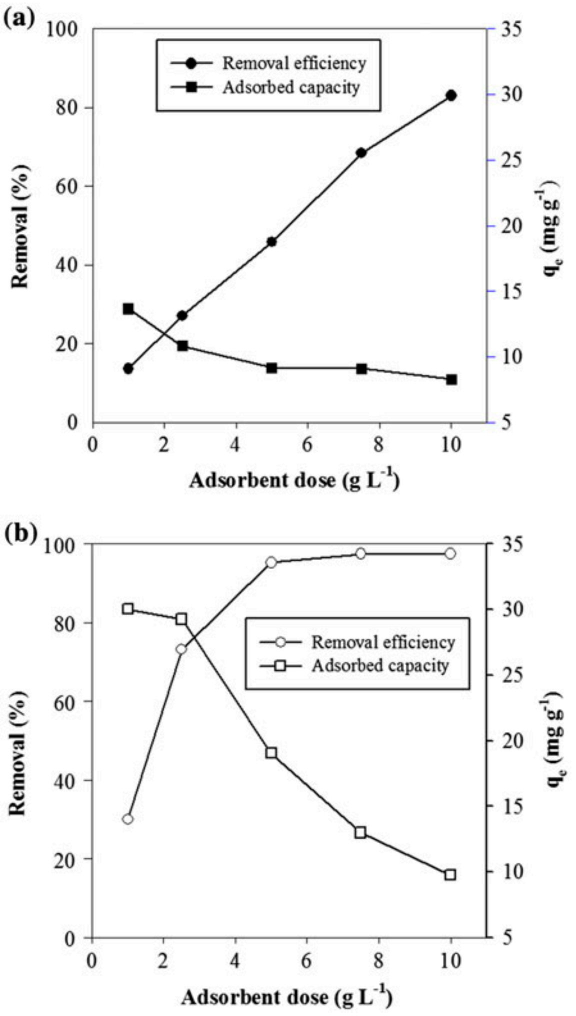

Fig. 3. Effect of adsorbent dose of DB (a) and NDB (b) on lead (II) removal.

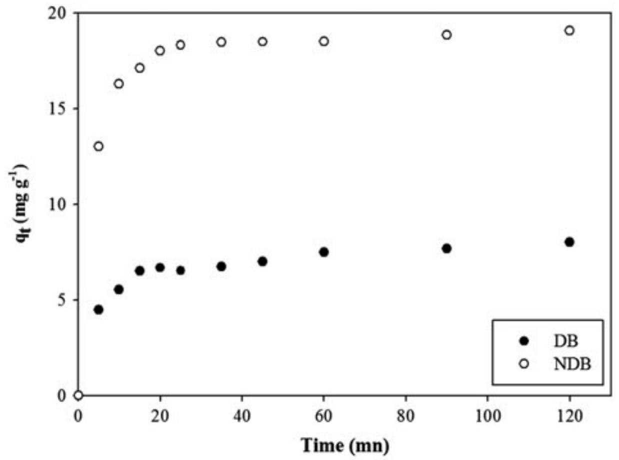

Fig. 4. Effect of contact time on amount of lead adsorbed on DB and NDB.

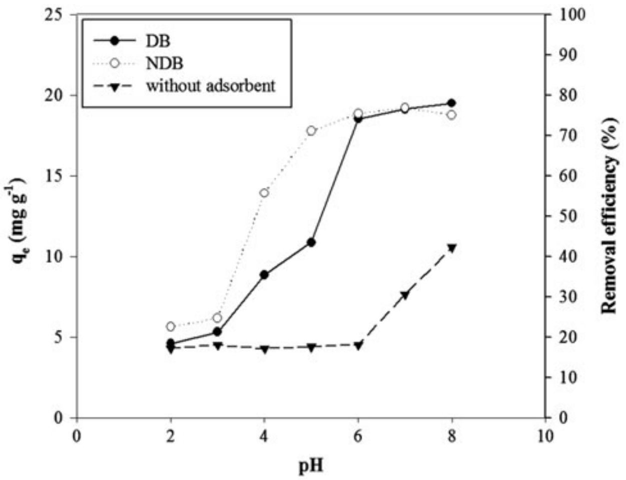

Fig. 5. Effect of pH on removal of lead from aqueous solution by DB and NDB.

and didn't show any particular change after this time. The NaOH treatment of DB stone enhanced the adsorption capacity, and a large amount of lead ions was removed in the first 20 min. This can be explained by the basis treatment performed by NaOH which improved the date stones surface with negative charge, increasing the electrostatic attraction between the cationic metal Pb(II) and the adsorbent NDB.

3.4. Effect of pH on Pb adsorption

The pH of the aqueous solution plays a major role in the adsorptive removal of heavy metals from aqueous solution. It can actually change the surface charge of an adsorbent and can also change the metal speciation [22,23]. Fig. 5 shows the effect of pH on the lead ions adsorption by DB, NDB with and without adsorbent (blank solutions of 100 mg L^{-1}). It is shown that the increase in the solution pH from 2 to 6 has a consequence enhancement of the adsorption capacity from 4.59 to 19.50 mg g^{-1} (corresponding to the removal percentages of 22.98–97.52%) for DB and from 5.59 to 19.21 mg g^{-1} (corresponding to the removal percentages of 27.98–96.08%) for NDB. At lower pH values, the low adsorption is due to the electrostatic repulsion and to the presence of excess of protons H$^+$ ions competing with Pb^{2+} cations for the exchange sites on the DB and NDB, which reduces the adsorbed amounts of lead ions. An increase pH shows an increase in adsorption up to 6, when the surface of DB and NDB becomes more negatively charged, resulting to the deprotonation of positively charged groups on

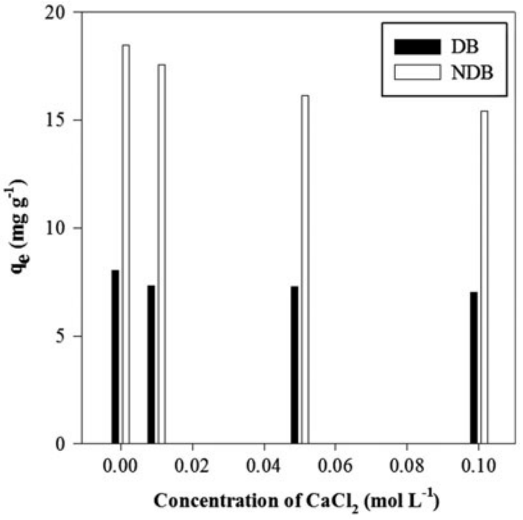

Fig. 6. Effect of ionic strength on adsorption.

the adsorbent surface. This deprotonation enhances electrostatic attraction between positively charged sorbate species [Pb^{2+} and $Pb(OH)^+$] and negative surface sites, increasing adsorption of lead on DB and NDB. At higher pH (pH > 6), the decrease in Pb^{2+} concentration in solution should be related to adsorption and precipitation (formation of $Pb(OH)_2$).

3.5. Effect of ionic strength on Pb(II) removal

Wastewaters contain various types of monovalent or divalent salt such as Na^+, K^+, Mg^{2+}, and Ca^{2+}. The presence of those cations in solution may enhance or adverse the performance of the adsorption process [24]. The influence of electrolyte concentration on the adsorption ability of the DB and NDB for lead (II) ions has been analyzed using $CaCl_2$ solutions with concentrations range from 0.0 to 0.1 mol L^{-1}. As shown in Fig. 6, it can be seen that, for an increase in divalent electrolyte concentration from 0.0 to 0.1 mol L^{-1}, the adsorption capacity of lead (II) ions decreased from 11.94 to 10.01 mg g^{-1} for DB and from 18.23 to 13.46 mg g^{-1} for NDB. This behavior can be explained assuming that the increase of the electrolyte concentration screens the electrostatic interaction of the opposite

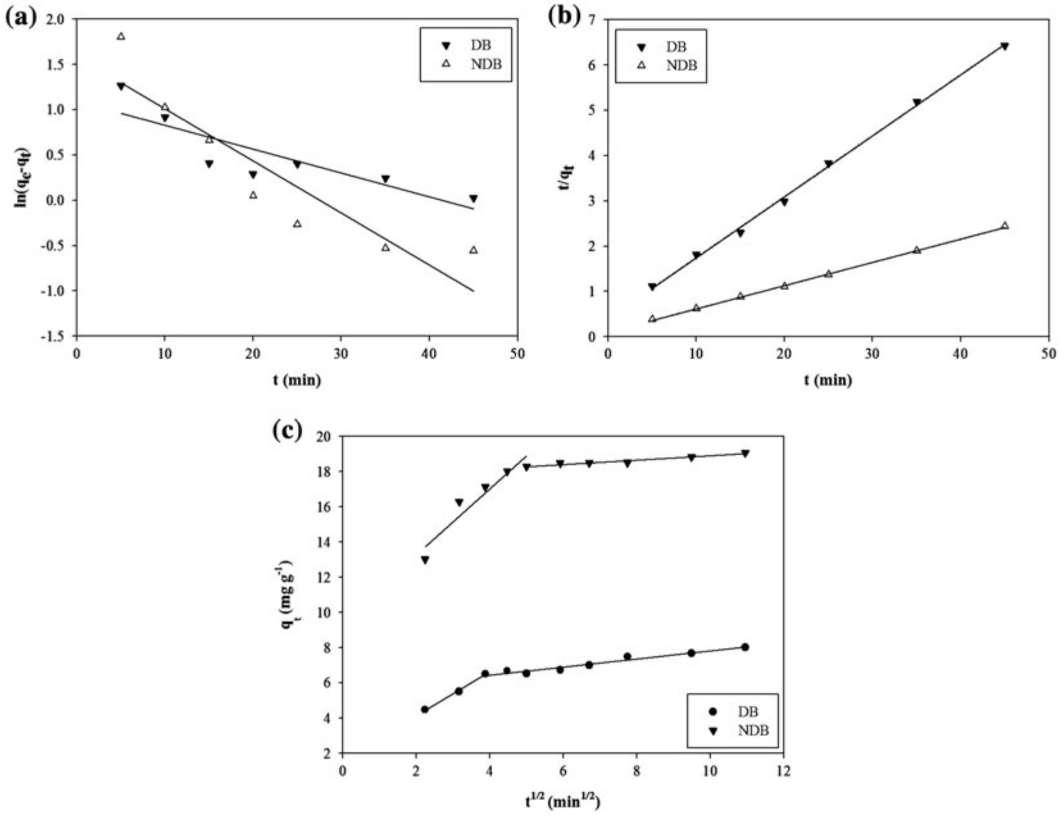

Fig. 7. Kinetic models of Pb(II) ions adsorption onto DB and NDB using (a) Pseudo-first-order model, (b) Pseudo-second-order model, and (c) Intraparticle diffusion.

Table 2
Kinetic model parameters for adsorption of lead(II) onto DB and NDB

			Pseudo-first-order model			Pseudo-second-order model		
Adsorbent	C_0 (mg L^{-1})	q_{exp} (mg g^{-1})	$q_{e,cal}$ (mg g^{-1})	k_1 (min^{-1})	R^2	$q_{e,cal}$ (mg g^{-1})	k_2 (g mg^{-1} min^{-1})	R^2
DB	100	08.02	02.98	0.026	0.747	07.42	0.175	0.998
NDB	100	19.08	04.86	0.172	0.832	19.49	0.025	0.999

Intraparticle diffusion model

Adsorbent	C_0 (mg L^{-1})	K_{id1} (mg g^{-1} $min^{-1/2}$)	C_1 (mg g^{-1})	R^2	K_{id2} (mg g^{-1} $min^{-1/2}$)	C_2 (mg g^{-1})	R^2
DB	100	1.241	1.666	0.995	0.225	5.554	0.952
NDB	100	1.862	9.571	0.908	0.122	17.68	0.949

charges on the adsorbent surface of the DB and NDB, causing a reduction in lead (II) ions adsorption.

3.6. Adsorption kinetics

Several kinetic models are used to provide valuable information on the mechanism that controls the adsorption process. Three different kinetic models, pseudo-first order, pseudo-second order, and intraparticle diffusion, were used to interpret the obtained experimental data [26,27]. The pseudo-first-order equation is represented by the following linear equation:

$$\ln(q_e - q_t) = \ln q_e - K_1 t \tag{3}$$

where k_1 (min^{-1}) is the rate constant of pseudo-first-order adsorption, q_t is the amount of lead ions adsorbed at time t (min), and q_e (mg g^{-1}) is the amount of lead ions adsorbed at equilibrium per unit weight of adsorbent. The slope and intercept of the plots of ln ($q_e - q_t$) vs. t was used to determine the first-order rate constant k_1 and q_e.

The pseudo-second-order is expressed by the following linear equation [25]:

$$\frac{t}{q_t} = \frac{1}{K_2 q_e^2} + \frac{1}{q_e} t \tag{4}$$

where q_t and q_e (mg g^{-1}) are the amounts of lead ions adsorbed at equilibrium per weight unit of adsorbent, respectively, k_2 (g mg^{-1} min^{-1}) is the pseudo-second-order rate constant.

The slope and intercept of the plot of t/q_e vs. t was used to determine the second-order rate constant k_2 and q_e.

The intraparticle diffusion model can be used to find the region where intraparticle diffusion is

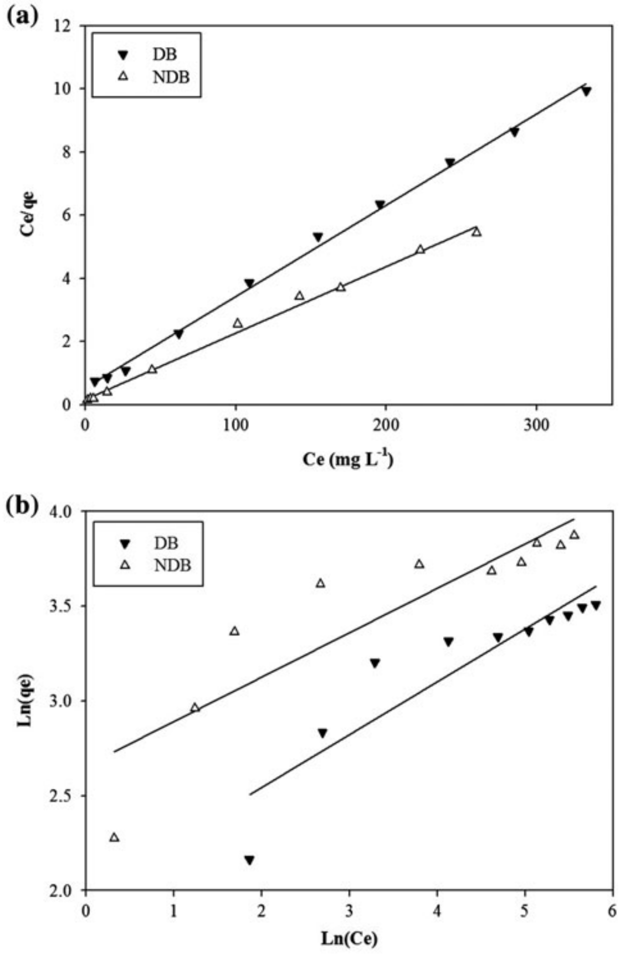

Fig. 8. Adsorption isotherm models for Pb(II) ions adsorption onto DB and NDB using: (a) Langmuir and (b) Freundlich.

rate-limited and also to determine intraparticle diffusion. In this model, the rate of intraparticle diffusion is function of $t^{1/2}$ and can be expressed as follows [26]:

$$q_t = K_{\mathrm{id}} t^{1/2} + C \tag{5}$$

where q_t (mg g^{-1}) is the amount adsorbed at time t (min), K_{id} is the intraparticle diffusion rate constant (mg g^{-1} min$^{-1/2}$), and C (milligram per gram) is the intercept which relates to the thickness of the boundary layer thickness. The slope K_{id} and intercept C were obtained by the plot of q_t vs. $t^{1/2}$.

Figs. 7(a)–(c) shows the comparison of pseudo-first-order model, pseudo-second-order model, and intraparticle diffusion, respectively, for Pb(II) ions adsorption onto DB and NDB. The values of kinetic parameters of all the kinetic models are included in Table 2. The results show that the pseudo-second-order model is the best in describing the kinetics of Pb (II) ions adsorbed onto DB and NDB compared to the pseudo-first-order model. The determination coefficients R^2 were found to be higher than 0.99 for DB and NDB. From the results, it is also seen that the values of ($q_{\mathrm{e,cal}}$) calculated from the pseudo-second-order model were nearest to the experimental values ($q_{\mathrm{e,exp}}$), indicating the applicability of this model to the adsorption of Pb(II) ions. This is based on the assumption that the rate limiting step may be chemisorption involving valence forces through sharing or exchange

Table 3
Equilibrium model parameters for adsorption of lead(II) onto DB and NDB

	Langmuir isotherm			Freundlich isotherm		
Adsorbent	$q_{\max}$ (mg g^{-1})	K_L (L mg^{-1})	R^2	K_F (L g^{-1})	$1/n$	R^2
DB	35.71	0.052	0.997	07.30	0.278	0.827
NDB	47.61	0.133	0.994	14.23	0.234	0.792

Table 4
Comparison of the maximal adsorption capacities Pb(II) ions obtained from various adsorbents

Adsorbent	Lead(II)	Refs.
Banana peel	02.18	Anwar and al. [33]
AAm/SMA	68.90	Krušić and al. [34]
Apricot stone activated carbon	21.38	Mouni and al. [35]
Al-MCM-41	14.50	Sepehrian and al. [36]
Bentonite	20.00	Naseem and Tahir [37]
Crab shell	19.83	Dahiya and al. [38]
Fly ash	15.08	Cho and al. [39]
Hazelnut shell	28.18	Pehlivan and al. [40]
Activated carbon of melocana	10.66	Lalhruaitluanga and al. [41]
Palm kernel fiber	32.50	Ho [27]
Tourmaline	20.83	He and al. [42]
Mansonia wood sawdust	51.81	Ofomaja [43]
Treated sawdust	52.38	Meena and al. [45]
Red mud	88.20	Gupta and al. [45]
Activated carbon of coconut shell (GCN1240)	92.39	Caccin and al. [46]
Activated carbon of coconut shell (GCN816G)	32.08	Caccin and al. [46]
Activated carbon of *Sea-buckthorn* Stones with H_3PO_4	51.81	Mohammadi and al. [47]
Activated carbon of *Sea-buckthorn* Stones with $ZnCl_2$	25.91	Mohammadi and al. [47]
Activated carbon of *Amygdalus Scoparia* shell with H_3PO_4	36.63	Mohammadi and al. [48]
Activated carbon *of Amygdalus Scoparia* shell with $ZnCl_2$	28.74	Mohammadi and al. [48]
Activated carbon *Glycyrrhiza glabra* residue with $ZnCl_2$	200	Mohammadi and al. [49]
Degla beida stone	35.71	Present study
Treated Degla beida stone	47.61	Present study

of electrons between adsorbent and adsorbate [27,28]. The Fig. 7(c) presents a multi-linearity relation where none of the lines passed through the origin, indicating that more than one process affects the Pb(II) ions adsorption [29].

3.7. Adsorption isotherms

Adsorption isotherm was used to obtain information about the mechanism and the interaction between the adsorbent and the adsorbate at a given temperature. The equilibrium adsorption experiments were analyzed by fitting them to Langmuir and Freundlich isotherm models. The linear form of the Langmuir (Eq. (6)) and Freundlich (Eq. (7)) isotherm equation is given as [30,31]:

$$\frac{C_e}{q_e} = \frac{1}{q_m K_L} + \frac{1}{q_m} C_e \tag{6}$$

$$\ln q_e = \ln K_F + \frac{1}{n} \ln C_e \tag{7}$$

where C_e (mg L^{-1}) is the equilibrium concentration of the adsorbate lead ions, q_e (mg g^{-1}) correspond to the amount of adsorbate adsorbed at equilibrium per unit mass of adsorbent, and q_m (mg g^{-1}) and K_L are Langmuir constant related to adsorption capacity and rate of adsorption, respectively. q_m and K_L are determined from the slope and the intercept of the plot of C_e/q_e vs. C_e. K_F and n are Freundlich constants, which correspond to the binding capacity and affinity between the sorbent and sorbate, respectively. The intercept and the slope are obtained from the slope of the linear plot of ln q_e against ln C_e. They provide the value of K_F and $1/n$. The characteristics of the Langmuir isotherm can be described by a distribution factor, defined as following [32]:

$$R_L = \frac{1}{1 + K_L C_0} \tag{8}$$

where R_L is the dimensionless equilibrium parameter and C_0 is the initial adsorbate concentration. The value of R_L indicates the type of isotherm. It can be either favorable when ($0 < R_L < 1$), unfavorable ($R_L > 1$), linear ($R_L = 1$), or irreversible ($R_L = 0$).

Fig. 8 shows a comparison between the linearized Langmuir and Freundlich isotherm models for lead (II) adsorption onto DB and NDB. According to the Table 3, the maximum adsorption capacity was 35.71 and 47.61 mg g^{-1} for the DB and NDB, respectively. Both adsorbents DB and NDB had better applicability for Langmuir isotherm model than Freundlich isotherm model, which confirms the monolayer adsorption and proves a surface homogeneity of the adsorbent. In addition to that, the values of R_L between 0 and 1 indicate favorable adsorption on DB and NDB. For comparison, the values of adsorption capacity of other adsorbents, taken from literature, are given in Table 4 for comparison.

4. Conclusion

This study concludes that untreated DB stone DB can be used for the removal of Pb(II) ions from water. Chemically pretreated DB stone NDB showed a better adsorption capacity than untreated DB from aqueous solutions, with an increase from 35.71 to 47.61 mg g^{-1}. Batch experiments showed that equilibrium data follow Langmuir isotherm. The rate of adsorption was found to be conformed to pseudo-second-order equation. The application of intra-particle diffusion model demonstrates that the adsorption onto DB and NDB followed multiple adsorption steps.

The obtained results indicate that DB and NDB can easily be used for the removal of Pb(II) ions from aqueous solution and this would be economically more viable, compared to other conventional treatments.

References

[1] F.M. Johnson, The genetic effects of environmental lead, Mutation Res. 410 (1998) 123–140.

[2] J.G. Lestón, J. Méndez, E. Pásaro, B. Laffon, Genotoxic effects of lead: An updated review, Environ. Int. 36 (2010) 623–636.

[3] M. Ahamed, M.K.J. Siddiqui, Environmental lead toxicity and nutritional factors, Clin. Nutr. 26 (2007) 400–408.

[4] M.M. Kadir, N.Z. Janjua, S. Kristensen, Z. Fatmi, N. Sathiakumar, Status of children's blood lead levels in Pakistan: Implications for research and policy, Publ. Health 122 (2008) 708–715.

[5] A. Ornek, M. Ozacar, I.A. Sengil, Adsorption of lead onto formaldehyde or sulphuric acid treated acorn waste: Equilibrium and kinetic studies, Biochem. Eng. J. 37 (2007) 192–200.

[6] S.S. Majumdar, S.K. Das, R. Chakravarty, T. Saha, T.S. Bandyopadhyay, A.K. Guha, A study on lead adsorption by Mucor rouxii biomass, Desalination 251 (2010) 96–102.

[7] X. Song, H. Liu, L. Cheng, Y. Qu, Surface modification of coconut-based activated carbon by liquid-phase oxidation and its effects on lead ion adsorption, Desalination 255 (2010) 78–83.

[8] M. Malakootian, J. Nouri, H. Hossaini, Removal of heavy metals from paint industry's wastewater using Leca as an available adsorbent, Int. J. Environ. Sci. Technol. 6 (2009) 183–190.

[9] P. Pengthamkeerati, T. Satapanajaru, N. Chatsatapattayakul, P. Chairattanamanokorn, N. Sananwai, Alkaline treatment of biomass fly ash for reactive dye removal from aqueous solution, Desalination 261 (2010) 34–40.

[10] M. Rafatullah, O. Sulaiman, R. Hashim, A. Ahmad, Adsorption of methylene blue on low-cost adsorbents: A review, J. Hazard. Mater. 177 (2010) 70–80.

[11] C. Namasivayam, N. Muniasamy, K. Gayatri, M. Rani, K. Ranganathan, Removal of dyes from aqueous solution by cellulosic waste orange peel, Bioresour. Technol. 57 (1996) 37–43.

[12] C. Namasivayam, D. Prabha, M. Kumutha, Removal of direct red and acid brilliant blue by adsorption onto banana pith, Bioresour. Technol. 64 (1998) 77–79.

[13] V.S. Mane, P.V.V. Babu, Studies on the adsorption of brilliant green dye from aqueous solution onto low-cost NaOH treated saw dust, Desalination 273 (2011) 321–329.

[14] D.J. Malik, V. Strelko Jr, M. Streat, A.M. Puziy, Characterisation of novel modified active carbons and marine algal biomass for the selective adsorption of lead, Water Res. 36 (2002) 1527–1538.

[15] A.K. Meena, G.K. Mishra, S. Kumar, C. Rajagopal, P.N. Nagar, Low-cost adsorbents for the removal of mercury (II) from aqueous solution–A comparative study, Defence Sci. J. 54 (2004) 537–548.

[16] S.R. Popuri, Y. Vijaya, V.M. Boddu, K. Abburi, Adsorptive removal of copper and nickel ions from water using chitosan coated PVC beads, Bioresour. Technol. 100 (2009) 194–199.

[17] S. Chakraborty, S. Chowdhury, P.D. Saha, Adsorption of crystal violet from aqueous solution onto NaOH-modified rice husk, Carbohydr. Polym. 86 (2011) 1533–1541.

[18] M.A. Shavandi, Z. Haddadian, M.H.S. Ismail, N. Abdullah, Z.Z. Abidin, Removal of residual oils from palm oil mill effluent by adsorption on natural zeolite, Water Air Soil Pollut. 223 (2012) 4017–4027.

[19] M.T. Uddin, M.A. Islam, S. Mahmud, M. Rukanuzzaman, Adsorptive removal of methylene blue by *tea* waste, J. Hazard. Mater. 164 (2009) 53–60.

[20] H. Lata, V.K. Garg, R.K. Gupta, Sequestration of nickel from aqueous solution onto activated carbon prepared from *Parthenium hysterophorus L*, J. Hazard. Mater. 157 (2008) 503–509.

[21] A. Somayajula, A. Abd Aziz, P. Saravanan, M. Matheswaran, Adsorption of mercury (II) ion from aqueous solution using low-cost activated carbon prepared from mango kernel, Asia-Pac. J. Chem. Eng. 8 (2013) 1–10.

[22] J.P. Huang, C.P. Huang, A.L. Morehart, Removal of Cu (II) from dilute aqueous solutions by Saccharomyces cerevisiae, Water Res. 24 (1990) 433–499.

[23] P. Miretzky, C. Munoz, Enhanced metal removal from aqueous by Fenton activated macrophyte biomass, Desalination 271 (2011) 20–28.

[24] Y. Liu, W. Wang, A. Wang, Adsorption of lead ions from aqueous solution by using carboxymethyl cellulose-g-poly (acrylic acid)/attapulgite hydrogel composites, Desalination 259 (2010) 258–264.

[25] Z.-Y. Yao, J.-H. Qi, L.-H. Wang, Equilibrium, kinetic and thermodynamic studies on the biosorption of Cu (II) onto chestnut shell, J. Hazard. Mater. 174 (2010) 137–143.

[26] Y.S. Ho, A.E. Ofomaja, Effects of calcium competition on lead sorption by palm kernel fibre, J. Hazard. Mater. 120 (2005) 157–162.

[27] L. Deng, Y. Su, H. Su, X. Wang, X. Zhu, Sorption and desorption of lead (II) from wastewater by green algae Cladophora fascicularis, J. Hazard. Mater. 143 (2007) 220–225.

[28] S. Recillas, A. García, E. González, E. Casals, V. Puntes, A. Sánchez, X. Font, Use of CeO_2, TiO_2 and Fe_3O_4 nanoparticles for the removal of lead from water toxicity of nanoparticles and derived compounds, Desalination 277 (2011) 213–220.

[29] M. Ozacar, I.A. Sengil, H. Turkmenler, Equilibrium and kinetic data, and adsorption mechanism for adsorption of lead onto valonia tannin resin, Chem. Eng. J. 143 (2008) 32–42.

[30] M.C. Ncibi, B. Mahjoub, M. Seffen, Kinetic and equilibrium studies of methylene blue biosorption by Posidonia oceanica (L) fibres, J. Hazard. Mater. 139 (2007) 280–285.

[31] I.A.W. Tan, A.L. Ahmad, B.H. Hameed, Adsorption of basic dye on high-surface-area activated carbon prepared from coconut husk: Equilibrium, kinetic and thermodynamic studies, J. Hazard. Mater. 154 (2008) 337–346.

[32] M. Doğan, H. Abak, M. Alkan, Biosorption of methylene blue from aqueous solutions by Hazelnut Shells: Equilibrium, Parameters and Isotherms, Water Air Soil Pollut. 192 (2008) 141–153.

[33] J. Anwar, U. Shafique, S. Waheed-uz-Zaman, M. Salman, A. Dar, S. Anwar, Removal of Pb(II) and Cd(II) from water by adsorption on peels of banana, Bioresour. Technol. 101 (2010) 1752–1755.

[34] M.K. Krušić, N. Milosavljević, A. Debeljković, Ö.B. Üzüm, E. Karadağ, Removal of Pb^{2+} ions from water by poly (*Acrylamide-co-Sodium Methacrylate*) hydrogels, Water Air Soil Pollut. 223 (2012) 4355–4368.

[35] L. Mouni, D. Merabet, A. Bouzaza, L. Belkhiri, Adsorption of Pb(II) from aqueous solutions using activated carbon developed from *Apricot* stone, Desalination 276 (2011) 148–153.

[36] H. Sepehrian, R. Cheraghali, H.A. Abdi, P. Rezaei, Adsorption studies of lead on modified mesoporous Al-MCM-41, Ion Exch. Lett. 4 (2011) 1–6.

[37] R. Naseem, S.S. Tahir, Removal of Pb(II) from aqueous/acidic solutions by using bentonite as an adsorbent, Water Res. 35 (2001) 3982–3986.

[38] S. Dahiya, R.M. Tripathi, A.G. Hegde, Biosorption of lead and copper from aqueous solutions by pre-treated *crab* and *arca shell* biomass, Bioresour. Technol. 99 (2008) 179–187.

[39] H. Cho, D. Oh, K. Kim, A study on removal characteristics of heavy metals from aqueous solution by *fly ash*, J. Hazard. Mater. 127 (2005) 187–195.

[40] E. Pehlivan, T. Altun, S. Cetin, M.I. Bhanger, Lead sorption by waste biomass of *hazelnut* and *almond shell*, J. Hazard. Mater. 167 (2009) 1203–1208.

[41] H. Lalhruaitluanga, K. Jayaram, M.N.V. Prasad, K.K. Kumar, Pb(II) adsorption from aqueous solution by raw and activated charcoals of melocanna baccifera roxburgh (bamboo)–A comparative study, J. Hazard. Mater. 175 (2010) 311–318.

[42] D. He, G. Yin, F. Dong, W. Zhang, Q. Bian, Y. Si, Adsorption of lead (II), Copper (II) on tourmaline from Altai Mine in China's Sinkiang, Acta Geophys. Sinica 86 (2012) 423–429.

[43] A.E. Ofomaja, E.I. Unuabonah, N.A. Oladoja, Competitive modeling for the biosorptive removal of copper and lead ions from aqueous solution by Mansonia wood sawdust, Bioresour. Technol. 101 (2010) 3844–3852.

[44] A.K. Meena, K. Kadirvelu, G.K. Mishra, C. Rajagopal, P.N. Nagar, Adsorptive removal of heavy metals from aqueous solution by treated sawdust (Acacia arabica), J. Hazard. Mater. 150 (2008) 604–611.

[45] V.K. Gupta, M. Gupta, S. Sharma, Process development for the removal of lead and chromium from aqueous solutions using red mud–An aluminium industry waste, Water Res. 35 (2001) 1125–1134.

[46] M. Caccin, M. Giorgi, F. Giacobbo, M.D. Ros, L. Besozzi, M. Mariani, Removal of lead (II) from aqueous solutions by adsorption onto activated carbons prepared from coconut shell, Desalin. Water Treat. 57 (2016) 4557–4575.

[47] S.Z. Mohammadi, M.A. Karimi, D. Afzali, F. Mansouri, Removal of Pb(II) from aqueous solutions using activated carbon from Sea-buckthorn stones by chemical activation, Desalination 262 (2010) 86–93.

[48] S.Z. Mohammadi, M.A. Karimi, D. Afzali, F. Mansouri, Preparation and characterization of activated carbon from Amygdalus Scoparia shell by chemical activation and its application for removal of lead from aqueous solutions, Cent. Eur. J. Chem. 8 (2010) 1273–1280.

[49] S.Z. Mohammadi, H. Hamidian, Z. Moeinadini, High surface area-activated carbon from Glycyrrhiza glabra residue by $ZnCl_2$ activation for removal of Pb(II) and Ni(II) from water samples, J. Ind. Eng. Chem. 20 (2014) 4112–4118.